Digital Compensation of Cross-Modulation Distortion in Software-Defined Radios

Qiyue Zou, *Member, IEEE*, Mohyee Mikhemar, *Student Member, IEEE*, and Ali H. Sayed, *Fellow, IEEE*

***Abstract*—The wideband RF receiver in a software-defined radio (SDR) system suffers from the nonlinear effects caused by the front-end analog processing. In the presence of strong blocker (interference) signals, such nonlinearities introduce severe cross modulation over the desired signals. This paper investigates how the cross-modulation distortion can be compensated for by using digital signal processing techniques. In the proposed solution, the SDR scans the wide spectrum and locates the desired signal and strong blocker signals. After down-converting these signals separately to the baseband, the baseband processor processes them jointly to mitigate the cross-modulation interferences. As a result, the sensitivity of the wideband RF receiver to the nonlinearity impairment can be significantly lowered, simplifying the RF and analog circuitry design in terms of implementation cost and power consumption. The proposed approach also demonstrates how mixed-signal, i.e., joint analog and digital, processing techniques play a critical role in the emerging SDR and cognitive radio technologies.**

***Index Terms*—Channel estimation, cross modulation, mixed-signal processing, nonlinearity, orthogonal frequency division multiplexing (OFDM), software-defined radio (SDR), wireless communication.**

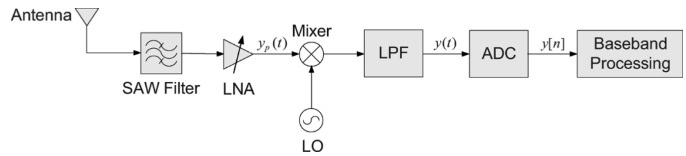

Fig. 1. Traditional receiver dedicated to the frequency band with carrier frequency ω_c.

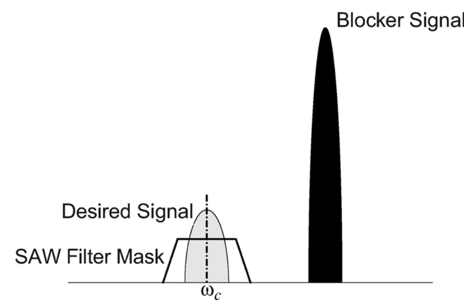

Fig. 2. SAW filter can effectively remove the strong blocker signals in other frequency bands.

I. Introduction

A software-defined radio (SDR) system is a radio communication system that can tune to any frequency band and receive any modulation across a large frequency spectrum by means of programmable hardware [2]–[6]. SDR systems allow the feasibility of different wireless services by using just a single reconfigurable chipset. Moreover, SDR systems offer a platform for the newly emerging cognitive radio technology, which demands high controllability and programmability for radio transmission and reception [7], [8]. The convenience and promise of SDR face numerous challenges. Traditionally, in order to simultaneously communicate over different frequency bands, the receiver uses several RF front-end modules so that signals in different bands can be received and processed separately. Fig. 1 shows an RF receiver dedicated to a communication channel with carrier frequency ω_c. Because of the high out-of-band rejection characteristic of the band-selection surface acoustic wave (SAW) filter, interferences at other frequencies are suppressed and they cause little distortion to the desired signal (as demonstrated in Fig. 2), even in the presence of considerable front-end analog imperfections such as nonlinearities and IQ imbalances [9], [10]. Unlike conventional RF receivers, an SDR uses a wideband RF front-end module with several GHz bandwidth. A *tunable* synthesizer and mixer are used to lock in the desired frequency band and down-convert the signal to the baseband [11], [12]. Without the SAW filter,[1] all the signals and interferences existing in the wideband range are amplified and down-converted. Due to the unavoidable nonlinearity in the low-noise amplifier (LNA), the presence of strong blocker (interference) signals causes cross modulation over the desired signal. This threat becomes significantly harmful, especially when the desired signal is weak.

While analog/RF designers are striving to improve the linearity of RF receivers, there have been works in the literature to mitigate this impairment by using digital domain techniques [13]–[17]. These digital solutions provide a flexible alternative

[1]A SAW filter cannot be used here because it is application-specific with a fixed center frequency and bandwidth. Until now, there is no tunable SAW filter with sufficiently good performance. Furthermore, the SAW filter cannot be integrated on-chip with the receiver circuitry, which means that a multi-standard receiver with many SAW filters will be bulky and expensive.

Manuscript received June 01, 2008; revised February 10, 2009. Current version published May 15, 2009. This work was supported by the NSF under Awards ECS-0601266 and ECS-0725441. This work was presented in part at the 33rd IEEE International Conference on Acoustics, Speech, and Signal Processing (ICASSP), 2008 [1]. The associate editor coordinating the review of this manuscript and approving it for publication was Prof. Naofal Al-Dhahir.

Q. Zou was with the Electrical Engineering Department, University of California, Los Angeles, CA 90095 USA. He is now with the WiLinx Corporation, San Diego, CA 90025 USA (e-mail: eqyzou@gmail.com).

M. Mikhemar and A. H. Sayed are with the Electrical Engineering Department, University of California, Los Angeles, CA 90095, USA (e-mail: mohyee@ee.ucla.edu; sayed@ee.ucla.edu).

Color versions of one or more of the figures in this paper are available online at http://ieeexplore.ieee.org.

Digital Object Identifier 10.1109/JSTSP.2009.2020266

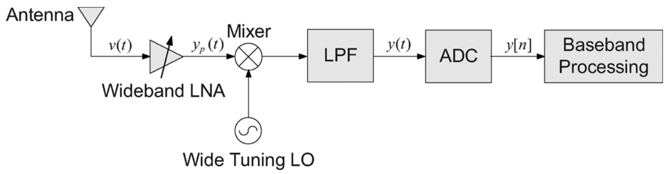

Fig. 3. SDR with a wideband front-end RF receiver [11], [12]. Without a SAW band-selection filter, the receiver acquires a wideband signal. The tunable oscillator and mixer are used to selectively down-convert the signal in a desired frequency band.

approach to combat nonlinearities, which is particularly appropriate for SDRs that have an extremely wide bandwidth and a reconfigurable hardware/software structure. In this paper, we propose a nonlinearity compensation scheme for the SDR structure proposed in [11], [12]. As shown in Fig. 3, this SDR system has a wideband RF front-end (0.8–6.0 GHz), and is able to selectively down-convert and sample the signals in desired frequency bands. Our scheme will require two RF signal paths—one is used for capturing the signal in the desired band, while the other is used to locate and acquire the blocker signal. The secondary RF path, used to acquire the blocker signal, can be implemented with smaller area and less power compared to the main path. As will be seen later, the proposed scheme only requires the information about the amplitude of the blocker signal, and hence adopts a relatively simple hardware implementation for the secondary path. The baseband processor jointly processes the two discretized signals to alleviate the effects of cross modulation.

The paper is organized as follows. The next section describes the system model and formulates the effects of RF nonlinearities when there exists only one blocker signal. The proposed compensation scheme is presented in Section III, and its performance is analyzed in Section IV in terms of the Cramer–Rao lower bound. Section V extends the system model and the proposed scheme to include multiple blocker signals as well as the orthogonal frequency division multiplexing (OFDM) transmission scheme. Simulation results are presented and discussed in Section VI.

Throughout this paper, we adopt the following notations. $(\cdot)^T$ denotes the matrix transpose and $(\cdot)^*$ represents the matrix conjugate transpose. $\mathrm{Re}\{\cdot\}$ and $\mathrm{Im}\{\cdot\}$ return the real and imaginary parts of its argument, respectively. $\mathbf{E}\{\cdot\}$ is the expected value with respect to the underlying probability measure, and $\mathrm{diag}\{\cdot\}$ represents the diagonal matrix whose diagonal entries are determined by its argument.

II. System Model

Referring to Fig. 3, in the presence of nonlinearities, the input–output characteristic of the receiver front-end is modeled as

$$y_p(t) = \alpha_1 v(t) + \alpha_2 [v(t)]^2 + \alpha_3 [v(t)]^3 + w_p(t) \quad (1)$$

where $v(t)$ and $y_p(t)$ are the real input and output signals, $w_p(t)$ is additive white Gaussian noise, and α_1, α_2, α_3 are real constants. In this expression, $\alpha_1 v(t)$ represents the linear component in the output, while $\alpha_2[v(t)]^2$ and $\alpha_3[v(t)]^3$ are the second and third-order nonlinear components in the output. The dynamic range of $v(t)$ depends on the sensitivity of the receive antenna. In this paper, the received signal power is assumed to be less than -20 dBm, and hence $v(t)$ is in the range [-0.032 V, 0.032 V], as shown by the following calculation:

$$\frac{|v(t)|^2}{2R} = -20 \text{ dBm} = 0.01 \text{ mW}$$

by which we can get $|v(t)| = 0.032$ V if $R = 50\ \Omega$. Practically speaking, the received power can be up to 0 dBm, which results in 10 times the voltage. Our work considers the signal level of -20 dBm because it corresponds to the 1-dB compression point of the receiver. The 1-dB compression point is about 10 dB below the IP3 (third-order intercept point) coefficient of the receiver, whose typical value is -10 dBm, i.e.,

$$-10 \text{ dBm} - 10 \text{ dB} = -20 \text{ dBm}.$$

For power levels larger than the 1-dB compression point, the gain compression will prevail and dominate the cross-modulation effect. The values of α_1, α_2 and α_3 are related to circuit specification parameters [9].

1) α_1 is the small signal gain and its typical value is 35 dB, i.e., $\alpha_1 = 56.23$.
2) α_2 is the coefficient representing the second-order nonlinearity, usually expressed in terms of the so-called IP2 (second-order intercept point) coefficient, i.e.,

$$\mathrm{IP2} = 20\log_{10}\frac{|\alpha_1|}{|\alpha_2|} + 10 \text{ (dBm)}$$

where dBm is the power ratio in decibels (dB) referenced to one milliwatt (mW). The typical value of IP2 is 30 dBm, implying that $\alpha_2 = \pm 5.623$ if $\alpha_1 = 56.23$.
3) α_3 is the coefficient representing the third-order nonlinearity, usually expressed in terms of the IP3 (third-order intercept point) coefficient, i.e.,

$$\mathrm{IP3} = 20\log_{10} V_{\mathrm{IP3}} + 10 \text{ (dBm)}$$

where

$$V_{\mathrm{IP3}} = \sqrt{\frac{4|\alpha_1|}{3|\alpha_3|}}.$$

The typical value of IP3 is -10 dBm, implying that $\alpha_3 = \pm 7497.33$ if $\alpha_1 = 56.23$.

For example, Fig. 4 plots $y_p(t)$ versus $v(t)$ for $\alpha_1 = 56.23$, $\alpha_2 = 5.623$, and $\alpha_3 = -7497.33$ according to (1).

Assume that the acquired signal $v(t)$ contains a desired signal around frequency ω_1 and a blocker signal around frequency ω_2.[2] Then, $v(t)$ can be represented by

$$v(t) = \mathrm{Re}\left\{\sqrt{2}z_1(t)e^{j\omega_1 t} + \sqrt{2}z_2(t)e^{j\omega_2 t}\right\} \quad (2)$$

where $z_1(t)$ and $z_2(t)$ are the corresponding baseband signals at ω_1 and ω_2. Taking the channel response of the desired channel

[2] We will discuss the presence of multiple blocker signals in Section V, which turns out to be a direct extension of this simple case.

into account, $z_1(t)$ is given by the convolution of the transmitted baseband signal $x_1(t)$ and the continuous-time baseband channel response $h(t)$, i.e.,

$$z_1(t) = \int_{-\infty}^{\infty} x_1(t-\tau)h(\tau)d\tau. \tag{3}$$

Substituting (2) into (1) gives

$$\begin{aligned}
y_p(t) =& \alpha_1 \mathrm{Re}\left\{\sqrt{2}z_1(t)e^{j\omega_1 t} + \sqrt{2}z_2(t)e^{j\omega_2 t}\right\} \\
&+ \alpha_2\left(\mathrm{Re}\left\{\sqrt{2}z_1(t)e^{j\omega_1 t} + \sqrt{2}z_2(t)e^{j\omega_2 t}\right\}\right)^2 \\
&+ \alpha_3\left(\mathrm{Re}\left\{\sqrt{2}z_1(t)e^{j\omega_1 t} + \sqrt{2}z_2(t)e^{j\omega_2 t}\right\}\right)^3 \\
&+ w_p(t) \\
=& \alpha_2 |z_1(t)|^2 + \alpha_2 |z_2(t)|^2 \\
&+ \mathrm{Re}\left\{\sqrt{2}\left(\alpha_1 z_1(t) + \frac{3\alpha_3}{2} z_1(t)|z_1(t)|^2 \right.\right. \\
&\qquad \left.\left. + 3\alpha_3 z_1(t)|z_2(t)|^2\right)e^{j\omega_1 t}\right\} \\
&+ \mathrm{Re}\left\{\sqrt{2}\left(\alpha_1 z_2(t) + \frac{3\alpha_3}{2} z_2(t)|z_2(t)|^2 \right.\right. \\
&\qquad \left.\left. + 3\alpha_3 |z_1(t)|^2 z_2(t)\right)e^{j\omega_2 t}\right\} \\
&+ \mathrm{Re}\left\{\sqrt{2}\left(\frac{\sqrt{2}\alpha_2}{2}[z_1(t)]^2\right)e^{j2\omega_1 t}\right\} \\
&+ \mathrm{Re}\left\{\sqrt{2}\left(\frac{\sqrt{2}\alpha_2}{2}[z_2(t)]^2\right)e^{j2\omega_2 t}\right\} \\
&+ \mathrm{Re}\left\{\sqrt{2}\left(\frac{\alpha_3}{2}[z_1(t)]^3\right)e^{j3\omega_1 t}\right\} \\
&+ \mathrm{Re}\left\{\sqrt{2}\left(\frac{\alpha_3}{2}[z_2(t)]^3\right)e^{j3\omega_2 t}\right\} \\
&+ \mathrm{Re}\left\{\sqrt{2}\left(\sqrt{2}\alpha_2 z_1(t)z_2(t)\right)e^{j(\omega_1+\omega_2)t}\right\} \\
&+ \mathrm{Re}\left\{\sqrt{2}\left(\sqrt{2}\alpha_2 z_1(t)z_2^*(t)\right)e^{j(\omega_1-\omega_2)t}\right\} \\
&+ \mathrm{Re}\left\{\sqrt{2}\left(\frac{3\alpha_3}{2}z_1(t)[z_2(t)]^2\right)e^{j(\omega_1+2\omega_2)t}\right\} \\
&+ \mathrm{Re}\left\{\sqrt{2}\left(\frac{3\alpha_3}{2}z_1(t)[z_2^*(t)]^2\right)e^{j(\omega_1-2\omega_2)t}\right\} \\
&+ \mathrm{Re}\left\{\sqrt{2}\left(\frac{3\alpha_3}{2}[z_1(t)]^2 z_2(t)\right)e^{j(2\omega_1+\omega_2)t}\right\} \\
&+ \mathrm{Re}\left\{\sqrt{2}\left(\frac{3\alpha_3}{2}[z_1(t)]^2 z_2^*(t)\right)e^{j(2\omega_1-\omega_2)t}\right\} \\
&+ w_p(t).
\end{aligned}$$

The produced signal components at different frequencies are listed in Table I. With proper down-conversion and low-pass filtering, the received baseband signal corresponding to the carrier frequency ω_1 is given by

$$y(t) = \alpha_1 z_1(t) + \frac{3\alpha_3}{2} z_1(t)|z_1(t)|^2 + 3\alpha_3 z_1(t)|z_2(t)|^2 + w(t)$$

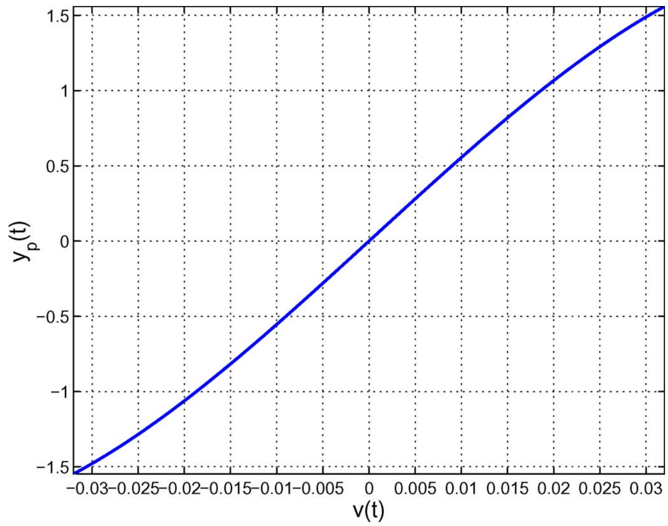

Fig. 4. Plot of the input–output relation—$y_p(t)$ versus $v(t)$ for $\alpha_1 = 56.23$, $\alpha_2 = 5.623$, and $\alpha_3 = -7497.33$.

TABLE I
TABLE OF THE SIGNAL COMPONENTS GENERATED BY THE NONLINEARITY MODEL (1)

Frequency	Signal Components
0	$\alpha_2|z_1(t)|^2 + \alpha_2|z_2(t)|^2$
ω_1	$\alpha_1 z_1(t) + \frac{3\alpha_3}{2} z_1(t)|z_1(t)|^2 + 3\alpha_3 z_1(t)|z_2(t)|^2$
ω_2	$\alpha_1 z_2(t) + \frac{3\alpha_3}{2} z_2(t)|z_2(t)|^2 + 3\alpha_3 |z_1(t)|^2 z_2(t)$
$2\omega_1$	$\frac{\sqrt{2}\alpha_2}{2}[z_1(t)]^2$
$2\omega_2$	$\frac{\sqrt{2}\alpha_2}{2}[z_2(t)]^2$
$3\omega_1$	$\frac{\alpha_3}{2}[z_1(t)]^3$
$3\omega_2$	$\frac{\alpha_3}{2}[z_2(t)]^3$
$\omega_1+\omega_2$	$\sqrt{2}\alpha_2 z_1(t)z_2(t)$
$\omega_1-\omega_2$	$\sqrt{2}\alpha_2 z_1(t)z_2^*(t)$
$\omega_1+2\omega_2$	$\frac{3\alpha_3}{2} z_1(t)[z_2(t)]^2$
$\omega_1-2\omega_2$	$\frac{3\alpha_3}{2} z_1(t)[z_2^*(t)]^2$
$2\omega_1+\omega_2$	$\frac{3\alpha_3}{2}[z_1(t)]^2 z_2(t)$
$2\omega_1-\omega_2$	$\frac{3\alpha_3}{2}[z_1(t)]^2 z_2^*(t)$

where $w(t)$ is the additive Gaussian noise in the baseband. This shows that $y(t)$ is distorted by the third-order harmonics $(3\alpha_3/2)z_1(t)|z_1(t)|^2$ and the cross-modulation term $3\alpha_3 z_1(t)|z_2(t)|^2$. If the amplitude of the desired signal is small, i.e., $|z_1(t)| \ll 1$, then the amplitude of $(3\alpha_3/2)z_1(t)|z_1(t)|^2$ is much smaller than that of $\alpha_1 z_1(t)$ and can be neglected. Its effect becomes significant only when the amplitude of $z_1(t)$ is close to 1, but can be mitigated by properly limiting the dynamic range of the input at little cost of loosing reception sensitivity. In a wideband SDR system, however, the cross modulation is more dangerous because of the blocker signal $z_2(t)$.[3] In real radio environments, the power of the blocker signal can be as much as 60–70 dB more than that of the desired signal. Since the receiver front-end has to maintain a minimum sensitivity level for the desired signal $z_1(t)$, then the simultaneously acquired blocker signal can be quite large,

[3]In a traditional narrow-band RF receiver, the blocker signal $z_2(t)$ is greatly suppressed by the SAW filter, and then the cross-modulation term is negligible.

making the interference term $3\alpha_3 z_1(t)|z_2(t)|^2$ comparable to the desired signal component $\alpha_1 z_1(t)$. To measure the effects quantitatively, the effective signal-to-noise ratio (SNR) in $y(t)$ is computed as (4) (see the equation at the bottom of the page), where $z_1(t)$, $z_2(t)$ and $w(t)$ are assumed to be zero-mean and independent of each other, and

$$\sigma_w^2 = \mathbf{E}\left\{|w(t)|^2\right\}$$

is the noise variance. In order to obtain a more explicit expression of $\mathrm{SNR}_{\mathrm{effective}}$, we consider the following two cases.

1) *Uniform Distribution*: Assume that the real and imaginary parts of $z_1(t)$ are i.i.d. uniformly distributed with mean zero, and the same for $z_2(t)$. This assumption approximates the case that $z_1(t)$ and $z_2(t)$ are PAM or QAM modulated in a single-carrier system. Let the variance of $z_i(t)$ be $\sigma_{z,i}^2$, $i = 1,\ 2$. It can be shown that (see Appendix A for a derivation)

$$\mathbf{E}\left\{|z_i(t)|^4\right\} = \frac{7}{5}\sigma_{z,i}^4, \quad \mathbf{E}\left\{|z_i(t)|^6\right\} = \frac{81}{35}\sigma_{z,i}^6 \tag{5}$$

for $i = 1,\ 2$. Let

$$\mathrm{SNR}_0 = \frac{\alpha_1^2\sigma_{z,1}^2}{\sigma_w^2}$$

be the effective signal-to-noise ratio in the absence of nonlinearity, i.e., $\alpha_2 = \alpha_3 = 0$. It follows from (4) that

$$\begin{aligned}\mathrm{SNR}_{\mathrm{effective}} &= \frac{\alpha_1^2\sigma_{z,1}^2}{\frac{729}{140}\alpha_3^2\sigma_{z,1}^6 + \frac{63}{5}\alpha_3^2\sigma_{z,1}^4\sigma_{z,2}^2 + \frac{63}{5}\alpha_3^2\sigma_{z,1}^2\sigma_{z,2}^4 + \sigma_w^2} \\ &= \frac{\mathrm{SNR}_0}{\frac{\alpha_3^2}{\alpha_1^2}\left(\frac{729}{140}\sigma_{z,1}^4 + \frac{63}{5}\sigma_{z,1}^2\sigma_{z,2}^2 + \frac{63}{5}\sigma_{z,2}^4\right)\mathrm{SNR}_0 + 1}. \end{aligned} \tag{6}$$

2) *Gaussian Distribution*: We now assume that $z_1(t)$ and $z_2(t)$ are circularly symmetric Gaussian distributed with mean zero and variance $\sigma_{z,1}^2$ and $\sigma_{z,2}^2$, respectively. This assumption approximates the scenario that $z_1(t)$ is an OFDM signal and $z_2(t)$ is a Gaussian interference. In this case

$$\mathbf{E}\left\{|z_i(t)|^4\right\} = 2\sigma_{z,i}^4, \quad \mathbf{E}\left\{|z_i(t)|^6\right\} = 6\sigma_{z,i}^6 \tag{7}$$

for $i = 1,\ 2$. Hence

$$\mathrm{SNR}_{\mathrm{effective}} = \frac{\mathrm{SNR}_0}{\frac{\alpha_3^2}{\alpha_1^2}\left(\frac{27}{2}\sigma_{z,1}^4 + 18\sigma_{z,1}^2\sigma_{z,2}^2 + 18\sigma_{z,2}^4\right)\mathrm{SNR}_0 + 1}. \tag{8}$$

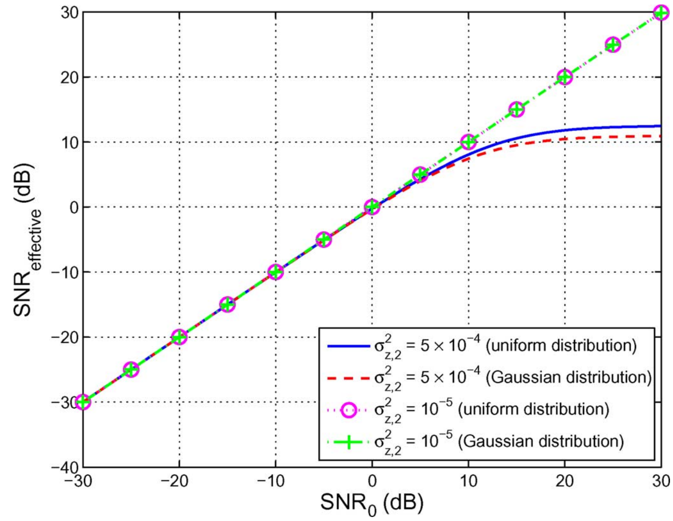

Fig. 5. Plot of $\mathrm{SNR}_{\mathrm{effective}}$ versus SNR_0 by (6) and (8) for $\alpha_1 = 56.23$, $\alpha_2 = 5.623$, $\alpha_3 = -7497.33$, and $\sigma_{z,1}^2 = 10^{-12}$.

Fig. 5 plots $\mathrm{SNR}_{\mathrm{effective}}$ versus SNR_0 for $\alpha_1 = 56.23$, $\alpha_2 = 5.623$, $\alpha_3 = -7497.33$, and $\sigma_{z,1}^2 = 10^{-12}$. When $\sigma_{z,2}^2 = 5\times10^{-4}$, for small SNR_0 the performance is noise-limited; but for large SNR_0, the performance is nonlinearity limited and the curve saturates. If the power of $z_2(t)$ changes to $\sigma_{z,2}^2 = 10^{-5}$ (17.0 dB less) and the other conditions remain the same, the resulting $\mathrm{SNR}_{\mathrm{effective}}$ is almost equal to SNR_0 and the nonlinearity causes no performance degradation. This observation demonstrates that a strong blocker signal can cause significant distortion to the desired signal. To overcome this problem, however, it is not feasible to limit the amplitude of the input signal $v(t)$ such that $z_2(t)$ is small, because this will also weaken the desired signal and, consequently, reduce the reception sensitivity. In the next section, we propose a compensation scheme to mitigate this effect by using digital signal processing techniques.

III. Proposed Compensation Scheme

In the proposed scheme, the SDR uses two separate RF signal paths. One path is used to capture the signal in the desired band, while the other path is used to acquire the blocker signal, as illustrated by Fig. 6. The desired signal path downconverts the desired signal around frequency ω_1 to the baseband, while the blocker signal path downconverts the blocker signal around frequency ω_2 to the baseband. The low-pass filters (LPF) extract

$$\begin{aligned}\mathrm{SNR}_{\mathrm{effective}} &= \frac{\mathbf{E}\left\{\alpha_1^2\,|z_1(t)|^2\right\}}{\mathbf{E}\left\{\left|\frac{3\alpha_3}{2}z_1(t)\,|z_1(t)|^2 + 3\alpha_3 z_1(t)\,|z_2(t)|^2 + w(t)\right|^2\right\}} \\ &= \frac{\alpha_1^2\mathbf{E}\left\{|z_1(t)|^2\right\}}{\frac{9\alpha_3^2}{4}\mathbf{E}\left\{|z_1(t)|^6\right\} + 9\alpha_3^2\mathbf{E}\left\{|z_1(t)|^4\right\}\mathbf{E}\left\{|z_2(t)|^2\right\} + 9\alpha_3^2\mathbf{E}\left\{|z_1(t)|^2\right\}\mathbf{E}\left\{|z_2(t)|^4\right\} + \sigma_w^2}\end{aligned} \tag{4}$$

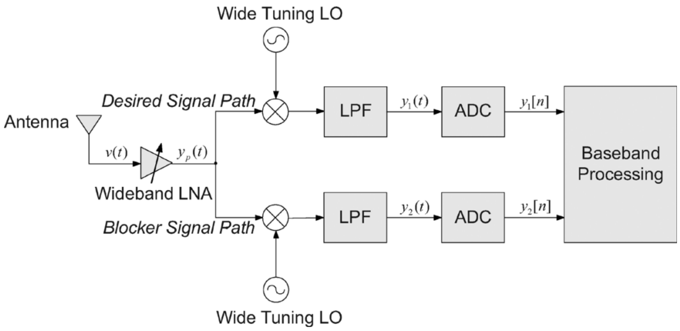

Fig. 6. Software-defined radio with two signal paths: one is used to capture the signal in the desired band, while the other is used to acquire the blocker signal.

the baseband version of the desired signal and the blocker signal before they are digitized by the ADCs. The two-channel signals are then jointly processed to alleviate the nonlinear effect. There are two stages in this scheme. In the first stage, the SDR exploits the pilot sequence in the desired signal to estimate the channel response and the nonlinearity parameters. These estimates are then used in the second stage to recover the transmitted data symbols. Since all wireless communication standards today provide pilot symbols at the beginning of every packet for synchronization and channel estimation, the proposed scheme does not require any modification to the packet structure and can be applied to existing standards. In the following discussion, we focus on the most problematic case of $\sigma_{z,1}^2 \ll \sigma_{z,2}^2$.

Before the channel and parameter estimation procedure, a robust synchronization procedure is performed in the desired channel for timing recovery. It is crucial for the receiver to be able to correctly sample each pilot or data symbol. The length of the synchronization sequence sent by the transmitter depends on the effective signal-to-noise ratio in the worst scenario. The lower the signal-to-noise ratio, the longer the training sequence is required [18]. In the presence of cross modulation, the effective signal-to-noise ratio is given by (6) and (8). The degradation thus requires a longer-than-normal training sequence for the system to operate in an adverse environment. After successful synchronization and sampling, we obtain the discrete-time version of the received baseband signals at the carrier frequencies ω_1 and ω_2

$$\begin{aligned} y_1[n] =& \alpha_1 z_1[n] + \frac{3\alpha_3}{2} z_1[n] \left| z_1[n] \right|^2 \\ &+ 3\alpha_3 z_1[n] \left| z_2[n] \right|^2 + w_1[n] \qquad (9) \\ y_2[n] =& \alpha_1' z_2[n] + \frac{3\alpha_3'}{2} z_2[n] \left| z_2[n] \right|^2 \\ &+ 3\alpha_3' \left| z_1[n] \right|^2 z_2[n] + w_2[n] \qquad (10) \end{aligned}$$

where α_1, α_3 are the model parameters associated with the desired signal path of $y_1(t)$, and α_1', α_3' are the model parameters associated with the blocker signal path of $y_2(t)$. Recall that in (3), $z_1(t)$ is given by the convolution of the baseband signal $x_1(t)$ and the continuous-time channel impulse response function $h(t)$. In the discrete-time domain, we have

$$z_1[n] = \sum_{l=0}^{L-1} x_1[n-l]h[l] \qquad (11)$$

where L is the length of $h[n]$, i.e., $h[n] = 0$ if $n \notin \{0, 1, \dots, L-1\}$.

In $y_1[n]$, since $|z_1[n]| \ll 1$, the third-order harmonics $(3\alpha_3/2)z_1[n]|z_1[n]|^2$ is negligible compared to the desired signal component $\alpha_1 z_1[n]$ and the cross-modulation term $3\alpha_3 z_1[n]|z_2[n]|^2$. Hence,

$$y_1[n] \approx \alpha_1 z_1[n] + 3\alpha_3 z_1[n] \left| z_2[n] \right|^2 + w_1[n]. \qquad (12)$$

Since $\sigma_{z,1}^2 \ll \sigma_{z,2}^2$ and $|z_2[n]| \ll 1$, the secondary-path signal $y_2[n]$ is dominated by $\alpha_1' z_2[n]$, i.e.,

$$y_2[n] \approx \alpha_1' z_2[n] + w_2[n] \qquad (13)$$

where $(3\alpha_3'/2)z_2[n]|z_2[n]|^2$ and $3\alpha_3'|z_1[n]|^2 z_2[n]$ are negligible compared to $\alpha_1' z_2[n]$.

A. Channel and Nonlinearity Parameter Estimation

In this stage, the receiver utilizes the pilot symbols transmitted along with the desired signal to estimate the channel response and the nonlinearity parameters. Thus, $x_1[n]$, $n = 0, 1, \dots, N-1$, are known to the receiver, where N is the length of the pilot sequence and $N > L$. By (12), α_1, α_3, and $h[n]$, $n = 0, 1, \dots, L-1$, can be estimated by solving the following optimization problem:

$$\min_{\alpha_1, \alpha_3, h[n]} \sum_{n=0}^{N-1} \left| y_1[n] - \alpha_1 z_1[n] - 3\alpha_3 z_1[n] \left| \widehat{z}_2[n] \right|^2 \right|^2$$

where $z_1[n]$ is related to $x_1[n]$ and $h[n]$ through (11) and $\widehat{z}_2[n]$ is given by

$$\widehat{z}_2[n] = \frac{1}{\alpha_1'} y_2[n]$$

according to (13). In this formulation, we have the product of α_1 and $z_1[n]$ and the product of α_3 and $z_1[n]|\widehat{z}_2[n]|^2$, which causes an ambiguity of a scaling factor in the estimate of α_1, α_3, and $h[n]$. To resolve this ambiguity, we estimate the following parameters instead:

$$\alpha_3'' = \frac{\alpha_3}{\alpha_1 \alpha_1'^2}$$

and

$$h''[n] = \alpha_1 h[n], \quad n = 0, 1, \dots, L-1.$$

The original problem thus becomes

$$\min_{\alpha_3'', h''[n]} \sum_{n=0}^{N-1} \left| y_1[n] - z_1''[n] - 3\alpha_3'' z_1''[n] \left| y_2[n] \right|^2 \right|^2$$

where

$$z_1''[n] = \sum_{l=0}^{L-1} x_1[n-l]h''[l]. \qquad (14)$$

This problem is nonlinear and nonconvex. For every *fixed* α_3'', the associated optimal $h''[n]$ can be obtained by solving

$$\min_{h''[n]} \sum_{n=0}^{N-1} \left| y_1[n] - z_1''[n] - 3\alpha_3'' z_1''[n] \, |y_2[n]|^2 \right|^2$$
$$= \min_{h''[n]} \sum_{n=0}^{N-1} \left| y_1[n] - \left(1 + 3\alpha_3'' |y_2[n]|^2\right) \left(\sum_{l=0}^{L-1} x_1[n-l] h''[l] \right) \right|^2$$

which can be formulated as a linear least-squares (LS) problem [19]

$$\min_{\mathbf{h}} \|\mathbf{y} - \mathbf{AXh}\|^2 \tag{15}$$

where $\mathbf{y}$, $\mathbf{h}$, $\mathbf{A}$, and $\mathbf{X}$ are defined as follows:

$$\mathbf{y} = \begin{bmatrix} y_1[0] \\ y_1[1] \\ \vdots \\ y_1[N-1] \end{bmatrix}, \; \mathbf{h} = \begin{bmatrix} h''[0] \\ h''[1] \\ \vdots \\ h''[L-1] \end{bmatrix}$$

$$\mathbf{A} = \mathrm{diag}\left\{ 1 + 3\alpha_3'' |y_2[0]|^2, 1 + 3\alpha_3'' |y_2[1]|^2, \ldots, 1 + 3\alpha_3'' |y_2[N-1]|^2 \right\}$$

$$\mathbf{X} = \begin{bmatrix} x_1[0] & 0 & \ldots & 0 \\ x_1[1] & x_1[0] & \ldots & 0 \\ \vdots & \vdots & \ddots & \vdots \\ x_1[n+L-1] & x_1[n+L-2] & \ldots & x_1[n] \\ x_1[n+L] & x_1[n+L-1] & \ldots & x_1[n+1] \\ \vdots & \vdots & \ddots & \vdots \\ x_1[N-2] & x_1[N-3] & \ldots & x_1[N-L-1] \\ x_1[N-1] & x_1[N-2] & \ldots & x_1[N-L] \end{bmatrix}.$$

The closed-form solution of (15) is

$$\mathbf{h}_{\mathrm{LS}} = (\mathbf{X}^*\mathbf{A}^*\mathbf{AX})^{-1}\mathbf{X}^*\mathbf{A}^*\mathbf{y}$$

and its associated residual error is

$$\|\mathbf{y} - \mathbf{AXh}_{\mathrm{LS}}\|^2 = \mathbf{y}^*\mathbf{y} - \mathbf{y}^*\mathbf{AX}(\mathbf{X}^*\mathbf{A}^*\mathbf{AX})^{-1}\mathbf{X}^*\mathbf{A}^*\mathbf{y}.$$

Note that the above residual error is a function of α_3'' because $\mathbf{A}$ depends on α_3''. Let

$$f_{\mathrm{LS}}(\alpha_3'') = \mathbf{y}^*\mathbf{y} - \mathbf{y}^*\mathbf{AX}(\mathbf{X}^*\mathbf{A}^*\mathbf{AX})^{-1}\mathbf{X}^*\mathbf{A}^*\mathbf{y}.$$

Then a one-dimensional search is conducted to find the optimal α_3'' that minimizes $f_{\mathrm{LS}}(\alpha_3'')$. That is, the estimate of α_3'' is given by

$$\widehat{\alpha}_3'' = \arg\min_{\alpha_3''} f_{\mathrm{LS}}(\alpha_3'')$$
$$= \arg\min_{\alpha_3''} \left\{ \mathbf{y}^*\mathbf{y} - \mathbf{y}^*\mathbf{AX}(\mathbf{X}^*\mathbf{A}^*\mathbf{AX})^{-1}\mathbf{X}^*\mathbf{A}^*\mathbf{y} \right\}.$$

The optimal $\mathbf{h}_{\mathrm{LS}}$ associated with $\widehat{\alpha}_3''$ gives an estimate of $h''[n]$, $n = 0, 1, \ldots, L-1$, that is denoted by $\widehat{h}''[n]$, $n = 0, 1, \ldots, L-1$. The obtained $\widehat{\alpha}_3''$ and $\widehat{h}''[n]$, $n = 0, 1, \ldots, L-1$, are used in the data transmission stage to recover data symbols.

If the receiver has information about the statistics of the channel response and the additive noise, the minimum-mean-square-error (MMSE) estimator can be used. Specifically, for every *fixed* α_3'', the associated optimal $h''[n]$ in the MMSE sense is given by [19]

$$\mathbf{h}_{\mathrm{MMSE}} = \mathbf{R}_{\mathbf{hy}}\mathbf{R}_{\mathbf{y}}^{-1}\mathbf{y} = \mathbf{R}_{\mathbf{h}}\mathbf{X}^*\mathbf{A}^*(\mathbf{AXR}_{\mathbf{h}}\mathbf{X}^*\mathbf{A}^* + \mathbf{R}_{\mathbf{w}})^{-1}\mathbf{y}$$

where

$$\mathbf{R}_{\mathbf{hy}} = \mathbf{E}\{\mathbf{hy}^*\}, \quad \mathbf{R}_{\mathbf{y}} = \mathbf{E}\{\mathbf{yy}^*\},$$
$$\mathbf{R}_{\mathbf{h}} = \mathbf{E}\{\mathbf{hh}^*\}, \quad \mathbf{R}_{\mathbf{w}} = \mathbf{E}\{\mathbf{ww}^*\}.$$

The estimate of α_3'' can be obtained by minimizing

$$f_{\mathrm{MMSE}}(\alpha_3'') = \|\mathbf{y} - \mathbf{AXh}_{\mathrm{MMSE}}\|^2$$

and the associated $\mathbf{h}_{\mathrm{MMSE}}$ gives the MMSE estimate of $h''[n]$, $n = 0, 1, \ldots, L-1$.

B. Data Symbol Estimation With Nonlinearity Compensation

In this stage, data symbols from a known constellation are transmitted over the channel. Since

$$y_1[n] \approx z_1''[n] + 3\widehat{\alpha}_3'' z_1''[n] \, |y_2[n]|^2 + w_1[n]$$
$$= \left(1 + 3\widehat{\alpha}_3'' |y_2[n]|^2\right) z_1''[n] + w_1[n]$$

the LS and MMSE estimates of $z_1''[n]$ are given by

$$\mathrm{LS}: \widehat{z}_1''[n] = \frac{y_1[n]}{1 + 3\widehat{\alpha}_3'' |y_2[n]|^2} \tag{16}$$

$$\mathrm{MMSE}: \widetilde{z}_1''[n] = \frac{y_1[n]}{1 + 3\widehat{\alpha}_3'' |y_2[n]|^2 + \frac{\sigma_{w_1}^2}{(1 + 3\widehat{\alpha}_3'' |y_2[n]|^2)\sigma_{z_1''}^2}} \tag{17}$$

where M is the length of the data symbol block, $\sigma_{w_1}^2 = \mathbf{E}\{|w_1[n]|^2\}$ and $\sigma_{z_1''}^2 = \mathbf{E}\{|z_1''[n]|^2\}$. It then follows from (14) that the estimate of $x_1[n]$ is given by

$$\widehat{x}_1[n] = \frac{1}{\widehat{h}''[0]} \left[\widehat{z}_1''[n] - \sum_{l=1}^{L-1} \widehat{x}_1[n-l] \widehat{h}''[l] \right]$$

where $\widehat{x}_1[n-l], l = 1, 2, \ldots, L-1$, are the previously estimated data symbols. This is similar to a decision-directed method. We can also recover $x_1[n]$ from $\widehat{z}_1''[n]$ by using an MMSE channel equalizer. If $x_1[n]$ are the symbols from a known constellation like QPSK or 16-QAM, the Viterbi algorithm can be exploited to obtain a more accurate estimate of $x_1[n]$ [20].

To gain an interpretation about the performance of the proposed algorithm, the data model can be rewritten as

$$y_1[n] = \left(\alpha_1 + 3\alpha_3 |z_2[n]|^2\right) z_1[n] + \frac{3\alpha_3}{2} z_1[n] \, |z_1[n]|^2 + w_1[n]$$

where $(\alpha_1+3\alpha_3|z_2[n]|^2)z_1[n]$ is the desired signal component[4] and $(3\alpha_3/2)z_1[n]|z_1[n]|^2+w_1[n]$ is the noise/interference term. The effective signal-to-noise ratio after compensation is approximately equal to the equation shown at the bottom of the page. If both $z_1[n]$ and $z_2[n]$ are uniformly distributed, by (5) we have

$$\begin{aligned}\mathrm{SNR}_{\mathrm{effective}} &= \frac{\left(\alpha_1^2+6\alpha_1\alpha_3\sigma_{z,2}^2+\frac{63}{5}\alpha_3^2\sigma_{z,2}^4\right)\sigma_{z,1}^2}{\frac{729}{140}\alpha_3^2\sigma_{z,1}^6+\sigma_w^2} \\ &= \frac{\left(1+\frac{6\alpha_3}{\alpha_1}\sigma_{z,2}^2+\frac{63\alpha_3^2}{5\alpha_1^2}\sigma_{z,2}^4\right)\mathrm{SNR}_0}{\frac{729\alpha_3^2}{140\alpha_1^2}\sigma_{z,1}^4\mathrm{SNR}_0+1}. \qquad (18)\end{aligned}$$

If both $z_1[n]$ and $z_2[n]$ are Gaussian distributed, by (7) we have

$$\begin{aligned}\mathrm{SNR}_{\mathrm{effective}} &= \frac{\left(\alpha_1^2+6\alpha_1\alpha_3\sigma_{z,2}^2+18\alpha_3^2\sigma_{z,2}^4\right)\sigma_{z,1}^2}{\frac{27}{2}\alpha_3^2\sigma_{z,1}^6+\sigma_w^2} \\ &= \frac{\left(1+\frac{6\alpha_3}{\alpha_1}\sigma_{z,2}^2+\frac{18\alpha_3^2}{\alpha_1^2}\sigma_{z,2}^4\right)\mathrm{SNR}_0}{\frac{27\alpha_3^2}{2\alpha_1^2}\sigma_{z,1}^4\mathrm{SNR}_0+1}. \qquad (19)\end{aligned}$$

Fig. 7 shows the plot of $\mathrm{SNR}_{\mathrm{effective}}$ versus SNR_0 after ideal compensation for $\alpha_1 = 56.23$, $\alpha_2 = 5.623$, $\alpha_3 = -7497.33$, $\sigma_{z,1}^2 = 10^{-12}$, and $\sigma_{z,2}^2 = 5\times 10^{-4}$. Compared to Fig. 5, it demonstrates that the compensation technique can achieve significant improvement. In the next section, we compute the Cramer–Rao lower bounds for the channel and data symbol estimation errors, which serve as a benchmark for evaluating the performance of the proposed algorithm.

IV. Performance Bounds

To evaluate the proposed algorithm, we compare its performance with the Cramer–Rao lower bound (CRLB) that gives a lower bound on the covariance matrix of any *unbiased* estimator of unknown parameters [21]. Consider the generic data model

$$\mathbf{y} = \mathbf{s}_{\boldsymbol{\theta}} + \mathbf{w}$$

where $\mathbf{y}$ is the observed data vector with length N, $\mathbf{s}_{\boldsymbol{\theta}}$ is the noise-free data vector that depends on the parameter vector $\boldsymbol{\theta}$, and $\mathbf{w}$ is the vector of circularly symmetric Gaussian noise with covariance matrix

$$\mathbf{E}\{\mathbf{w}\mathbf{w}^*\} = \mathrm{diag}\left\{\sigma_{w,0}^2, \sigma_{w,1}^2, \ldots, \sigma_{w,N-1}^2\right\}.$$

[4]It assumes that $z_2[n]$ can be ideally estimated and compensated for.

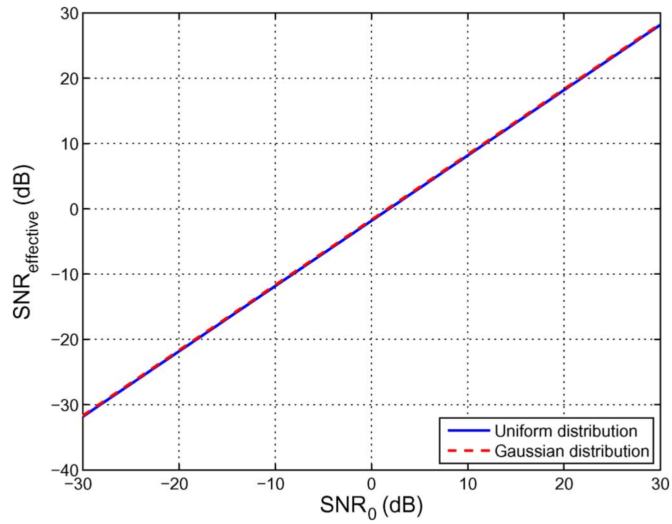

Fig. 7. Plot of $\mathrm{SNR}_{\mathrm{effective}}$ after ideal compensation versus SNR_0 by (18) and (19) for $\alpha_1 = 56.23$, $\alpha_2 = 5.623$, $\alpha_3 = -7497.33$, $\sigma_{z,1}^2 = 10^{-12}$, and $\sigma_{z,2}^2 = 5\times 10^{-4}$.

Let

$$\mathbf{s}_{\boldsymbol{\theta}} = [s_{\boldsymbol{\theta}}[0] \quad s_{\boldsymbol{\theta}}[1] \quad \ldots \quad s_{\boldsymbol{\theta}}[N-1]]^T.$$

The Fisher information matrix for this data model is given by (see [21])

$$\mathbf{I}_{\boldsymbol{\theta}} = \sum_{n=0}^{N-1}\frac{2}{\sigma_{w,n}^2}\mathrm{Re}\left\{\frac{\partial s_{\boldsymbol{\theta}}[n]}{\partial\boldsymbol{\theta}}\left(\frac{\partial s_{\boldsymbol{\theta}}[n]}{\partial\boldsymbol{\theta}}\right)^*\right\} \qquad (20)$$

where

$$\frac{\partial s_{\boldsymbol{\theta}}[n]}{\partial\boldsymbol{\theta}} = \left[\frac{\partial s_{\boldsymbol{\theta}}[n]}{\partial\theta_1} \quad \frac{\partial s_{\boldsymbol{\theta}}[n]}{\partial\theta_2} \quad \ldots \quad \frac{\partial s_{\boldsymbol{\theta}}[n]}{\partial\theta_{|\boldsymbol{\theta}|}}\right]^T$$

and $|\boldsymbol{\theta}|$ is the dimension of $\boldsymbol{\theta}$. By the CRLB, any unbiased estimator $\widehat{\boldsymbol{\theta}}$ of $\boldsymbol{\theta}$ has a covariance matrix that satisfies

$$\mathrm{var}\{\widehat{\boldsymbol{\theta}}\} = \mathbf{E}\left\{(\widehat{\boldsymbol{\theta}}-\boldsymbol{\theta})(\widehat{\boldsymbol{\theta}}-\boldsymbol{\theta})^*\right\} \geq \mathbf{I}_{\boldsymbol{\theta}}^{-1} \qquad (21)$$

where $\mathrm{var}\{\widehat{\boldsymbol{\theta}}\} \geq \mathbf{I}_{\boldsymbol{\theta}}^{-1}$ is interpreted as meaning that the matrix $\mathrm{var}\{\widehat{\boldsymbol{\theta}}\} - \mathbf{I}_{\boldsymbol{\theta}}^{-1}$ is positive semidefinite.

$$\begin{aligned}\mathrm{SNR}_{\mathrm{effective}} &\approx \frac{\mathbf{E}\left\{\left|\left(\alpha_1+3\alpha_3\left|z_2[n]\right|^2\right)z_1[n]\right|^2\right\}}{\mathbf{E}\left\{\left|\frac{3\alpha_3}{2}z_1[n]\left|z_1[n]\right|^2+w_1[n]\right|^2\right\}} \\ &= \frac{\left(\alpha_1^2+6\alpha_1\alpha_3\mathbf{E}\left\{\left|z_2[n]\right|^2\right\}+9\alpha_3^2\mathbf{E}\left\{\left|z_2[n]\right|^4\right\}\right)\mathbf{E}\left\{\left|z_1[n]\right|^2\right\}}{\frac{9}{4}\alpha_3^2\mathbf{E}\left\{\left|z_1[n]\right|^6\right\}+\sigma_w^2}.\end{aligned}$$

A. CRLB for Estimating Channel Response and Nonlinearity Parameters

The data model described by (9) and (10) is equivalent to

$$\begin{aligned} y_1[n] &= z_1''[n] + 3\alpha_3'' z_1''[n]\left|z_2''[n]\right|^2 \\ &\quad + \frac{3\alpha_3}{2} z_1[n]\left|z_1[n]\right|^2 + w_1[n] \end{aligned} \tag{22}$$

$$\begin{aligned} y_2[n] &= z_2''[n] + \frac{3\alpha_3'}{2} z_2[n]\left|z_2[n]\right|^2 \\ &\quad + 3\alpha_3'\left|z_1[n]\right|^2 z_2[n] + w_2[n] \end{aligned} \tag{23}$$

where $z_2''[n] = \alpha_1' z_2[n]$. The model can be expressed as

$$\begin{aligned} y_1[n] &= s_{\boldsymbol{\theta},1}[n] + w_1'[n] \\ y_2[n] &= s_{\boldsymbol{\theta},2}[n] + w_2'[n] \end{aligned}$$

where the noise-free signal components $s_{\boldsymbol{\theta},1}[n]$ and $s_{\boldsymbol{\theta},2}[n]$ are given by

$$\begin{aligned} s_{\boldsymbol{\theta},1}[n] &= z_1''[n] + 3\alpha_3'' z_1''[n]\left|z_2''[n]\right|^2 \\ s_{\boldsymbol{\theta},2}[n] &= z_2''[n] \end{aligned}$$

and the noise components $w_1'[n]$ and $w_2'[n]$ are given by

$$\begin{aligned} w_1'[n] &= \frac{3\alpha_3}{2} z_1[n]\left|z_1[n]\right|^2 + w_1[n] \\ w_2'[n] &= \frac{3\alpha_3'}{2} z_2[n]\left|z_2[n]\right|^2 + 3\alpha_3'\left|z_1[n]\right|^2 z_2[n] + w_2[n]. \end{aligned}$$

We assume that $w_1'[n]$ and $w_2'[n]$ are approximately Gaussian distributed with variances

$$\begin{aligned} \sigma_{w_1'}^2 &= \mathbf{E}\left\{\left|\frac{3\alpha_3}{2} z_1[n]\left|z_1[n]\right|^2 + w_1[n]\right|^2\right\} \\ &= \frac{9\alpha_3^2}{4}\mathbf{E}\left\{\left|z_1[n]\right|^6\right\} + \sigma_w^2 \\ &= \begin{cases} \frac{729\alpha_3^2}{140}\sigma_{z,1}^6 + \sigma_w^2, & \text{if } z_1(t) \text{ is uniformly distributed} \\ \frac{27\alpha_3^2}{2}\sigma_{z,1}^6 + \sigma_w^2, & \text{if } z_1(t) \text{ is Gaussian distributed} \end{cases} \end{aligned}$$

and as shown in the equation at the bottom of the page. The unknown parameter vector to be estimated is

$$\begin{aligned} \boldsymbol{\theta} = [\alpha_3'' \;\; &\mathrm{Re}\{h''[0]\} \;\; \mathrm{Im}\{h''[0]\} \;\; \ldots \\ &\mathrm{Re}\{h''[L-1]\} \;\; \mathrm{Im}\{h''[L-1]\} \\ &\mathrm{Re}\{z_2''[0]\} \;\; \mathrm{Im}\{z_2''[0]\} \;\; \ldots \\ &\mathrm{Re}\{z_2''[N-1]\} \;\; \mathrm{Im}\{z_2''[N-1]\}]^T. \end{aligned}$$

By (20), the Fisher information matrix is given by

$$\mathbf{I}_{\boldsymbol{\theta}} = \sum_{m=1}^{2}\sum_{n=0}^{N-1}\frac{2}{\sigma_{w_m'}^2}\mathrm{Re}\left\{\frac{\partial s_{\boldsymbol{\theta},m}[n]}{\partial\boldsymbol{\theta}}\left(\frac{\partial s_{\boldsymbol{\theta},m}[n]}{\partial\boldsymbol{\theta}}\right)^*\right\} \tag{24}$$

where

$$\begin{aligned} \frac{\partial s_{\boldsymbol{\theta},m}[n]}{\partial\boldsymbol{\theta}} = \Bigg[&\frac{\partial s_{\boldsymbol{\theta},m}[n]}{\partial\alpha_3''} \;\; \frac{\partial s_{\boldsymbol{\theta},m}[n]}{\partial\mathrm{Re}\{h''[0]\}} \;\; \frac{\partial s_{\boldsymbol{\theta},m}[n]}{\partial\mathrm{Im}\{h''[0]\}} \;\; \ldots \\ &\frac{\partial s_{\boldsymbol{\theta},m}[n]}{\partial\mathrm{Re}\{h''[L-1]\}} \;\; \frac{\partial s_{\boldsymbol{\theta},m}[n]}{\partial\mathrm{Im}\{h''[L-1]\}} \\ &\frac{\partial s_{\boldsymbol{\theta},m}[n]}{\partial\mathrm{Re}\{z_2''[0]\}} \;\; \frac{\partial s_{\boldsymbol{\theta},m}[n]}{\partial\mathrm{Im}\{z_2''[0]\}} \;\; \ldots \\ &\frac{\partial s_{\boldsymbol{\theta},m}[n]}{\partial\mathrm{Re}\{z_2''[N-1]\}} \;\; \frac{\partial s_{\boldsymbol{\theta},m}[n]}{\partial\mathrm{Im}\{z_2''[N-1]\}}\Bigg]^T \end{aligned}$$

for $m = 1, 2$. It can be shown that for $n = 0, 1, \ldots, N-1$

$$\begin{aligned} \frac{\partial s_{\boldsymbol{\theta},1}[n]}{\partial\alpha_3''} &= 3z_1''[n]\left|z_2''[n]\right|^2 \\ \frac{\partial s_{\boldsymbol{\theta},1}[n]}{\partial\mathrm{Re}\{h''[l]\}} &= x_1[n-l] + 3\alpha_3'' x_1[n-l]\left|z_2''[n]\right|^2 \\ \frac{\partial s_{\boldsymbol{\theta},1}[n]}{\partial\mathrm{Im}\{h''[l]\}} &= jx_1[n-l] + j3\alpha_3'' x_1[n-l]\left|z_2''[n]\right|^2 \\ \frac{\partial s_{\boldsymbol{\theta},1}[n]}{\partial\mathrm{Re}\{z_2''[n']\}} &= \begin{cases} 3\alpha_3'' z_1''[n'] \\ \quad\times\left[z_2''[n'] + (z_2''[n'])^*\right], & \text{if } n = n' \\ 0, & \text{if } n \neq n' \end{cases} \\ \frac{\partial s_{\boldsymbol{\theta},1}[n]}{\partial\mathrm{Im}\{z_2''[n']\}} &= \begin{cases} j3\alpha_3'' z_1''[n'] \\ \quad\times\left[-z_2''[n'] + (z_2''[n'])^*\right], & \text{if } n = n' \\ 0, & \text{if } n \neq n' \end{cases} \end{aligned}$$

and

$$\frac{\partial s_{\boldsymbol{\theta},2}[n]}{\partial\alpha_3''} = 0 \qquad \frac{\partial s_{\boldsymbol{\theta},2}[n]}{\partial\mathrm{Re}\{h''[l]\}} = 0 \qquad \frac{\partial s_{\boldsymbol{\theta},2}[n]}{\partial\mathrm{Im}\{h''[l]\}} = 0$$

$$\begin{aligned} \frac{\partial s_{\boldsymbol{\theta},2}[n]}{\partial\mathrm{Re}\{z_2''[n']\}} &= \begin{cases} 1, & \text{if } n = n' \\ 0, & \text{if } n \neq n' \end{cases} \\ \frac{\partial s_{\boldsymbol{\theta},2}[n]}{\partial\mathrm{Im}\{z_2''[n']\}} &= \begin{cases} j, & \text{if } n = n' \\ 0, & \text{if } n \neq n'. \end{cases} \end{aligned}$$

For each particular α_1, α_3, $h[n]$, $n = 0, 1, \ldots, L-1$, and training sequence $x_1[n]$, $n = 0, 1, \ldots, N-1$, the associated Fisher information matrix and the CRLB can be computed by using (24) and (21), respectively. An average is then taken over the ensemble of all possible channel realizations to get the average CRLB for the estimation errors.

$$\begin{aligned} \sigma_{w_2'}^2 &= \mathbf{E}\left\{\left|\frac{3\alpha_3'}{2} z_2[n]\left|z_2[n]\right|^2 + 3\alpha_3'\left|z_1[n]\right|^2 z_2[n] + w_2[n]\right|^2\right\} \\ &= \frac{9}{4}\left(\alpha_3'\right)^2\mathbf{E}\left\{\left|z_2[n]\right|^6\right\} + 9\left(\alpha_3'\right)^2\mathbf{E}\left\{\left|z_1[n]\right|^2\right\}\mathbf{E}\left\{\left|z_2[n]\right|^4\right\} + 9\left(\alpha_3'\right)^2\mathbf{E}\left\{\left|z_1[n]\right|^4\right\}\mathbf{E}\left\{\left|z_2[n]\right|^2\right\} + \sigma_w^2 \\ &= \begin{cases} \frac{729\left(\alpha_3'\right)^2}{140}\sigma_{z,2}^6 + \frac{63\left(\alpha_3'\right)^2}{5}\sigma_{z,1}^2\sigma_{z,2}^4 + \frac{63\left(\alpha_3'\right)^2}{5}\sigma_{z,1}^4\sigma_{z,2}^2 + \sigma_w^2, & \text{if } z_1(t) \text{ is uniformly distributed} \\ \frac{27\left(\alpha_3'\right)^2}{2}\sigma_{z,2}^6 + 18\left(\alpha_3'\right)^2\sigma_{z,1}^2\sigma_{z,2}^4 + 18\left(\alpha_3'\right)^2\sigma_{z,1}^4\sigma_{z,2}^2 + \sigma_w^2, & \text{if } z_1(t) \text{ is Gaussian distributed.} \end{cases} \end{aligned}$$

B. CRLB for Estimating Data Symbols

In this case, the data model is still given by (22) and (23), but the unknown parameter vector to be estimated changes to

$$\begin{aligned}\boldsymbol{\theta} = [&\mathrm{Re}\{z_1''[0]\} \;\; \mathrm{Im}\{z_1''[0]\} \;\; \ldots \\ &\mathrm{Re}\{z_1''[M-1]\} \;\; \mathrm{Im}\{z_1''[M-1]\} \\ &\mathrm{Re}\{z_2''[0]\} \;\; \mathrm{Im}\{z_2''[0]\} \;\; \ldots \\ &\mathrm{Re}\{z_2''[M-1]\} \;\; \mathrm{Im}\{z_2''[M-1]\}]^T.\end{aligned}$$

The Fisher information matrix is given by

$$\mathbf{I}_{\boldsymbol{\theta}} = \sum_{m=1}^{2}\sum_{n=0}^{N-1}\frac{2}{\sigma_{w_m'}^2}\mathrm{Re}\left\{\frac{\partial s_{\boldsymbol{\theta},m}[n]}{\partial\boldsymbol{\theta}}\left(\frac{\partial s_{\boldsymbol{\theta},m}[n]}{\partial\boldsymbol{\theta}}\right)^*\right\}$$

where $\partial s_{\boldsymbol{\theta},m}[n]/\partial\boldsymbol{\theta}$ is now defined as

$$\begin{aligned}\frac{\partial s_{\boldsymbol{\theta},m}[n]}{\partial\boldsymbol{\theta}} = \Bigg[&\frac{\partial s_{\boldsymbol{\theta},m}[n]}{\partial\mathrm{Re}\{z_1''[0]\}} \;\; \frac{\partial s_{\boldsymbol{\theta},m}[n]}{\partial\mathrm{Im}\{z_1''[0]\}} \;\; \ldots \\ &\frac{\partial s_{\boldsymbol{\theta},m}[n]}{\partial\mathrm{Re}\{z_1''[M-1]\}} \;\; \frac{\partial s_{\boldsymbol{\theta},m}[n]}{\partial\mathrm{Im}\{z_1''[M-1]\}} \\ &\frac{\partial s_{\boldsymbol{\theta},m}[n]}{\partial\mathrm{Re}\{z_2''[0]\}} \;\; \frac{\partial s_{\boldsymbol{\theta},m}[n]}{\partial\mathrm{Im}\{z_2''[0]\}} \;\; \ldots \\ &\frac{\partial s_{\boldsymbol{\theta},m}[n]}{\partial\mathrm{Re}\{z_2''[M-1]\}} \;\; \frac{\partial s_{\boldsymbol{\theta},m}[n]}{\partial\mathrm{Im}\{z_2''[M-1]\}}\Bigg]^T \\ &m = 1, 2.\end{aligned}$$

For $n = 0, 1, \ldots, M-1$, it is easy to verify that

$$\begin{aligned}\frac{\partial s_{\boldsymbol{\theta},1}[n]}{\partial\mathrm{Re}\{z_1''[n']\}} &= \begin{cases}1 + 3\alpha_3''\left|z_2''[n]\right|^2, & \text{if } n = n'\\ 0, & \text{if } n \neq n'\end{cases}\\ \frac{\partial s_{\boldsymbol{\theta},1}[n]}{\partial\mathrm{Im}\{z_1''[n']\}} &= \begin{cases}j + j3\alpha_3''\left|z_2''[n]\right|^2, & \text{if } n = n'\\ 0, & \text{if } n \neq n'\end{cases}\\ \frac{\partial s_{\boldsymbol{\theta},1}[n]}{\partial\mathrm{Re}\{z_2''[n']\}} &= \begin{cases}3\alpha_3'' z_1''[n'] \\ \quad\times\left(z_2''[n'] + (z_2''[n'])^*\right), & \text{if } n = n'\\ 0, & \text{if } n \neq n'\end{cases}\\ \frac{\partial s_{\boldsymbol{\theta},1}[n]}{\partial\mathrm{Im}\{z_2''[n']\}} &= \begin{cases}j3\alpha_3'' z_1''[n'] \\ \quad\times\left(-z_2''[n'] + (z_2''[n'])^*\right), & \text{if } n = n'\\ 0, & \text{if } n \neq n'\end{cases}\end{aligned}$$

and

$$\begin{aligned}&\frac{\partial s_{\boldsymbol{\theta},2}[n]}{\partial\mathrm{Re}\{z_1''[n']\}} = 0 \qquad \frac{\partial s_{\boldsymbol{\theta},2}[n]}{\partial\mathrm{Im}\{z_1''[n']\}} = 0\\ &\frac{\partial s_{\boldsymbol{\theta},2}[n]}{\partial\mathrm{Re}\{z_2''[n']\}} = \begin{cases}1, & \text{if } n = n'\\ 0, & \text{if } n \neq n'\end{cases}\\ &\frac{\partial s_{\boldsymbol{\theta},2}[n]}{\partial\mathrm{Im}\{z_2''[n']\}} = \begin{cases}j, & \text{if } n = n'\\ 0, & \text{if } n \neq n'.\end{cases}\end{aligned}$$

In Section VI, we compare the simulated estimation errors with the computed CRLB, and show that the CRLB provides a good theoretical measure of the estimation accuracy. The next section extends the current discussion to the cases of multiple blocker signals and OFDM modulated transmission.

V. Some Extensions

A. Multiple Blocker Signals

In the presence of multiple blocker signals, the received passband signal is represented by

$$v(t) = \mathrm{Re}\left\{\sum_{k=1}^{K}\sqrt{2}z_k(t)e^{j\omega_k t}\right\}$$

where $z_1(t)$ is the desired signal and $z_k(t), k = 2, 3, \ldots, K$, are the blocker signals with

$$\mathbf{E}\left\{\left|z_1(t)\right|^2\right\} \ll \mathbf{E}\left\{\left|z_k(t)\right|^2\right\}, \quad k = 2, 3, \ldots, K.$$

Assume that the SDR has K RF paths with each dedicated to one of the carrier frequencies ω_k, $k = 1, 2, \ldots, K$. Similar to (9) and (10), it can be shown that the received baseband signals are

$$\begin{aligned}y_1[n] = \alpha_1 z_1[n] &+ \frac{3\alpha_3}{2}z_1[n]\left|z_1[n]\right|^2 \\ &+ 3\alpha_3\sum_{k'=2}^{K}z_1[n]\left|z_{k'}[n]\right|^2 + w_1[n]\end{aligned}$$

and

$$\begin{aligned}y_k[n] = \alpha_{1,k}' z_k[n] &+ \frac{3\alpha_{3,k}'}{2}z_k[n]\left|z_k[n]\right|^2 + 3\alpha_{3,k}' \\ &\cdot\sum_{k'=1,k'\neq k}^{K}z_k[n]\left|z_{k'}[n]\right|^2 + w_k[n], \quad k = 2, 3, \ldots, K\end{aligned}$$

where $\alpha_{1,k}'$ and $\alpha_{3,k}'$ are the nonlinear model parameters associated with the signal path of $y_k(t)$, $k = 2, 3, \ldots, K$. To estimate the model parameters and the channel response in the training stage, we use the following approximations:

$$y_1[n] \approx \alpha_1 z_1[n] + 3\alpha_3\sum_{k'=2}^{K}z_1[n]\left|z_{k'}[n]\right|^2 + w_1[n] \quad (25)$$

$$y_k[n] \approx \alpha_{1,k}' z_k[n] + w_k[n], \; k = 2, 3, \ldots, K. \quad (26)$$

Expression (26) leads to

$$\hat{z}_k[n] \approx \frac{1}{\alpha_{1,k}'}y_k[n], \quad k = 2, 3, \ldots, K.$$

By substitution, (25) becomes

$$y_1[n] \approx \alpha_1 z_1[n] + 3\sum_{k'=2}^{K}\frac{\alpha_3}{\alpha_{1,k'}'^2}z_1[n]\left|y_{k'}[n]\right|^2 + w_1[n].$$

Let $z_1''[n] = \alpha_1 z_1[n]$ and $\alpha_{3,k}'' = \alpha_3/\alpha_1\alpha_{1,k}'^2$. Hence,

$$y_1[n] \approx z_1''[n] + 3\sum_{k'=2}^{K}\alpha_{3,k'}'' z_1''[n]\left|y_{k'}[n]\right|^2 + w_1[n].$$

The same technique presented in Section III-A can be used to estimate $\alpha''_{3,k}$, $k = 2, 3, \ldots, K$, and $h''[n]$, $n = 0, 1, \ldots, L-1$, where the matrix $\mathbf{A}$ is now given by

$$\mathbf{A} = \mathrm{diag}\left\{1 + 3\sum_{k'=2}^{K} \alpha''_{3,k'} \left|y_{k'}[0]\right|^2, \ldots, \right. \\ \left. 1 + 3\sum_{k'=2}^{K} \alpha''_{3,k'} \left|y_{k'}[N-1]\right|^2 \right\}$$

and the search for optimal $\alpha''_{3,k}$, $k = 2, 3, \ldots, K$, is conducted in a $(K-1)$-dimensional space. In the data transmission stage, $z''_1[n]$ can be similarly estimated by the equation shown at the bottom of the page.

B. OFDM Systems

In OFDM systems, the pilot and data symbols are transmitted in the frequency domain. Let $X_1[k]$, $k = 0, 1, \ldots, N-1$, be the frequency components to be transmitted using the N subcarriers of the OFDM modulator. They are converted to the time-domain symbols $x_1[n]$, $n = 0, 1, \ldots, N-1$, by the inverse fast Fourier transform (IFFT). With the aid of the cyclic prefix, linear convolution becomes circular convolution in the discrete-time domain, i.e.,

$$z_1[n] = \sum_{l=0}^{L-1} x_1\left[(n-l)_N\right] h[l], \quad n = 0, 1, \ldots, N-1 \quad (27)$$

where $(n-l)_N$ stands for $(n-l) \bmod N$. At the receiver, the received time-domain symbols $y_1[n]$ are given by (9). The unitary fast Fourier transform (FFT) is performed on $y_1[n]$, $n = 0, 1, \ldots, N-1$, to obtain $Y_1[k]$, $k = 0, 1, \ldots, N-1$. In the absence of nonlinearity, i.e., $\alpha_3 = 0$, we have

$$Y_1[k] = H''[k]X_1[k] + W_1[k], \quad k = 0, 1, \ldots, N-1 \quad (28)$$

where $H''[k]$ is the channel response in the k^{th} subcarrier and $W_1[k]$ is the additive noise in the k^{th} subcarrier. Note that $H''[k]$, $k = 0, 1, \ldots, N-1$, are the Fourier transform coefficients of $h''[n] = \alpha_1 h[n]$, $n = 0, 1, \ldots, L-1$. If $H''[k]$ is known at the receiver, $X_1[k]$ can be estimated based on the relationship (28). In the presence of cross modulation, expression (28) becomes invalid. To compensate for the distortion, the proposed time-domain algorithm in Section III is applied before the OFDM demodulation. In the channel estimation stage, the frequency-domain pilot symbols $X_1[k]$, $k = 0, 1, \ldots, N-1$, and hence $x_1[n]$, $n = 0, 1, \ldots, N-1$, are known to the receiver, and because of the circular convolution (27), the channel estimation algorithm presented in Section III-A is applied with $\mathbf{X}$ modified to

$$\mathbf{X} = \begin{bmatrix} x_1[0] & x_1[N-1] & \ldots & x_1[N-L+1] \\ x_1[1] & x_1[0] & \ldots & x_1[N-L+2] \\ \vdots & \vdots & \ddots & \vdots \\ x_1[N-2] & x_1[N-3] & \ldots & x_1[N-L-1] \\ x_1[N-1] & x_1[N-2] & \ldots & x_1[N-L] \end{bmatrix}.$$

The obtained time-domain channel response $\widehat{h}''[n]$, $n = 0, 1, \ldots, L-1$, is converted to the frequency-domain response $\widehat{H}''[k]$, $k = 0, 1, \ldots, N-1$, for OFDM demodulation. In the data transmission stage, we first estimate $z''_1[n]$ in the time domain by (16) or (17). The FFT is applied on $\widehat{z}''_1[n]$ to obtain $\widehat{Z}''_1[k]$ and the frequency-domain transmitted symbols $X_1[k]$ are estimated by

$$\mathrm{LS}: \widehat{X}_1[k] = \frac{\widehat{Z}''_1[k]}{\widehat{H}''[k]}, \quad k = 0, 1, \ldots, N-1$$

$$\mathrm{MMSE}: \widehat{X}_1[k] = \frac{\widehat{Z}''_1[k]}{\widehat{H}''[k] + \frac{\sigma^2_{X_1}}{\left(\widehat{H}''[k]\right)^* \sigma^2_{W_1}}}$$
$$k = 0, 1, \ldots, N-1$$

where $\sigma^2_{X_1} = \mathbf{E}\{|X_1[k]|^2\}$ and $\sigma^2_{W_1} = \mathbf{E}\{|W_1[k]|^2\}$.

VI. Computer Simulations

In the simulations, the bandwidth of the desired signal and blocker signals is 20 MHz, and the constellation used for the desired signal is QPSK. The channel response is modeled as an FIR filter with length 4, and its taps are independently Rayleigh distributed with the total power normalized to be 1. We first simulate the single-carrier system when there is only one blocker signal. The average received signal power is set to be $\sigma^2_{z,1} = 10^{-12}$ and $\sigma^2_{z,2} = 5 \times 10^{-4}$. The model parameters of the desired channel and the blocker signal channels are specified as $\alpha_1 = 56.23$, $\alpha_2 = 5.623$, $\alpha_3 = -7497.33$, $\alpha'_1 = 0.5623$, $\alpha'_2 = 0.0005623$, and $\alpha'_3 = -0.00749733$. Compared to the desired channel, this is equivalent to a 40-dB attenuation in the blocker signal channel. The analysis in Section II shows that the desired channel is distorted by the cross modulation, but the secondary channel is still dominated by the blocker signal. The channel estimation method proposed in Section III-A uses pilot sequences of length 16 or 64, and its normalized mean-square-error (MSE) and CRLB are plotted versus the normalized signal-to-noise ratio at the receiver, i.e., $\mathrm{SNR}_0 = \alpha_1^2\sigma^2_{z,1}/\sigma^2_w$, in Fig. 8. It can

$$\mathrm{LS}: \widehat{z}''_1[n] = \frac{y_1[n]}{1 + 3\sum_{k'=2}^{K} \widehat{\alpha}''_{3,k'} \left|y_{k'}[n]\right|^2},$$

$$\mathrm{MMSE}: \widehat{z}''_1[n] = \frac{y_1[n]}{1 + 3\sum_{k'=2}^{K} \widehat{\alpha}''_{3,k'} \left|y_{k'}[n]\right|^2 + \frac{\sigma^2_{w_1}}{\left(1+3\sum_{k'=2}^{K} \widehat{\alpha}''_{3,k'} |y_{k'}[n]|^2\right)\sigma^2_{z''_1}}}.$$

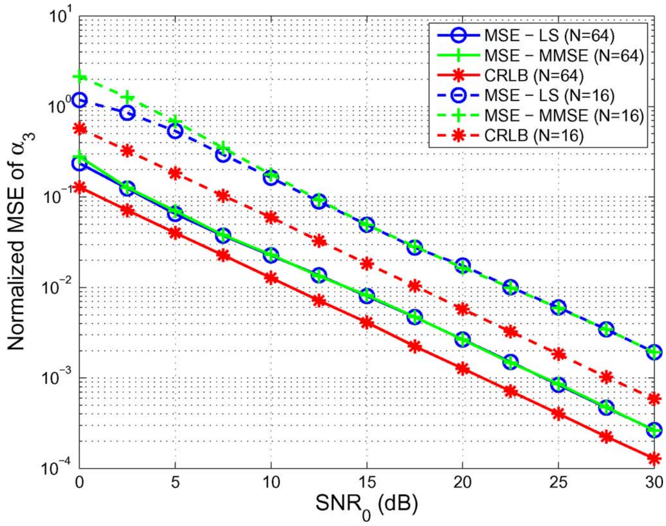

(a)

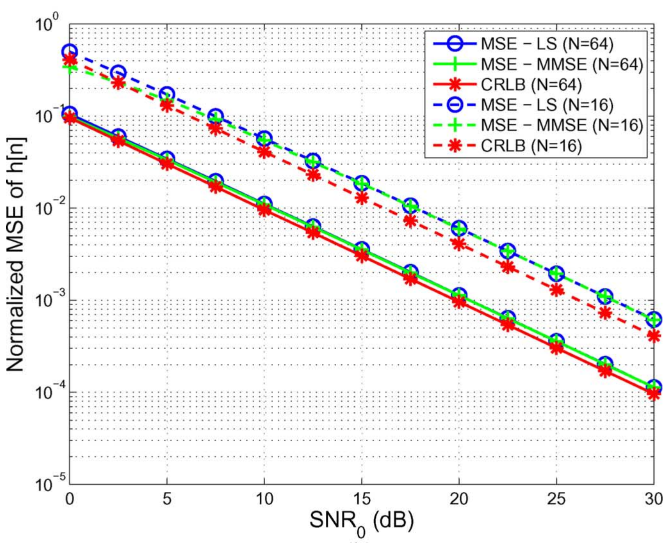

(b)

Fig. 8. Plots of the normalized mean-square-error (MSE) and Cramer–Rao lower bound (CRLB) for channel estimation when $\alpha_1 = 56.23$, $\alpha_2 = 5.623$, $\alpha_3 = -7497.33, \sigma_{z,1}^2 = 10^{-12}$, and $\sigma_{z,2}^2 = 5 \times 10^{-4}$. (a) MSE and CRLB of α_3. (b) MSE and CRLB of $\mathbf{h}$.

be seen that the CRLB provides a good measure of the estimation accuracy. Fig. 9 shows the MSE performance of the data symbol estimation algorithm proposed in Section III-B when assuming that the receiver has perfect knowledge of the model parameters and the channel response. Fig. 10 compares the BER performance of the whole proposed scheme, i.e., including both channel estimation and data symbol estimation, with that of a distorted receiver without any compensation. The Viterbi algorithm is used to demodulate the estimated QPSK symbols into information bits. It shows in Figs. 9 and 10 that the effective signal-to-noise ratio after compensation is about 27.5 dB. Since the effective signal-to-noise ratio depends on α_3 according to (6) and (8), the effective α_3 and IP3 can be computed accordingly. For the 27.5-dB effective signal-to-noise ratio, we find that the effective IP3 is about -0.72 dBm and so the improvement in the effective IP3 is -0.72 dBm $- (-10)$ dBm $= 9.28$ dB.

Fig. 11 shows the BER plots of the proposed scheme when there are two blocker signals with $\sigma_{z,2}^2 = \sigma_{z,3}^2 = 2.5 \times 10^{-4}$.

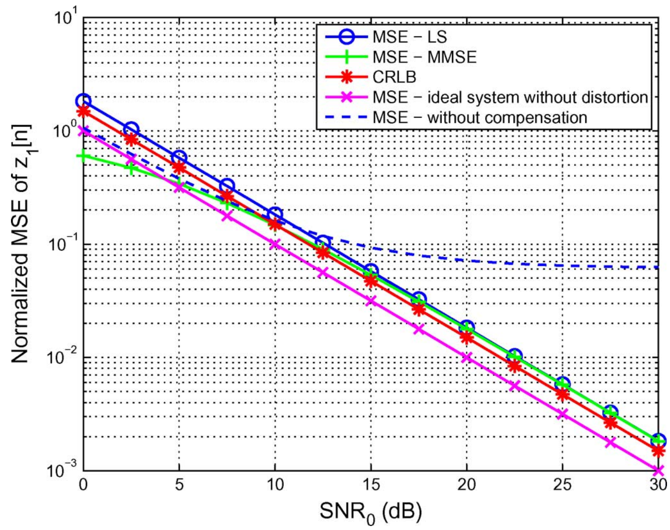

Fig. 9. Plots of the normalized mean-square error (MSE) and Cramer–Rao lower bound (CRLB) for data symbol estimation when $\alpha_1 = 56.23$, $\alpha_2 = 5.623, \alpha_3 = -7497.33, \sigma_{z,1}^2 = 10^{-12}$, and $\sigma_{z,2}^2 = 5 \times 10^{-4}$.

The performance is close to that shown in Fig. 10, because the total powers of the blocker signals are the same in the two cases. In Fig. 12, we demonstrate the performance of an OFDM system with 64 subcarriers and cyclic prefix length 16. The channel response is still modeled as an FIR filter with length 4, and each tap is Rayleigh distributed. Without any compensation, the system performs poorly and saturates at a high BER. The proposed compensation scheme improves the performance significantly.

VII. Conclusion

In this paper, the effects of RF nonlinearities in a software-defined radio (SDR) receiver are studied. A compensation scheme is proposed that consists of two stages. One stage is the joint channel and nonlinearity parameter estimation, and the other is the data symbol estimation via distortion compensation. The proposed channel estimation algorithm performs close to the derived Cramer–Rao lower bound. Also, the analysis and simulations show that the compensation scheme can effectively improve the system performance and reduce the sensitivity of SDR receivers to the nonlinearity impairment. Since receivers with less analog impairments usually have the disadvantage of high implementation cost and power consumption, our techniques enable the use of low-cost receivers for the next-generation wireless communications that are built on the platform of SDRs.

Appendix A
Derivation of Expressions (5) and (7)

Denote the real and imaginary parts of $z_i(t)$ by $z_{i,R}(t)$ and $z_{i,I}(t)$, respectively. Since $z_i(t)$ is zero-mean, its variance is given by

$$\sigma_{z,i}^2 = \mathbf{E}\left\{|z_i(t)|^2\right\} = \mathbf{E}\left\{z_{i,R}^2(t)\right\} + \mathbf{E}\left\{z_{i,I}^2(t)\right\}. \quad (29)$$

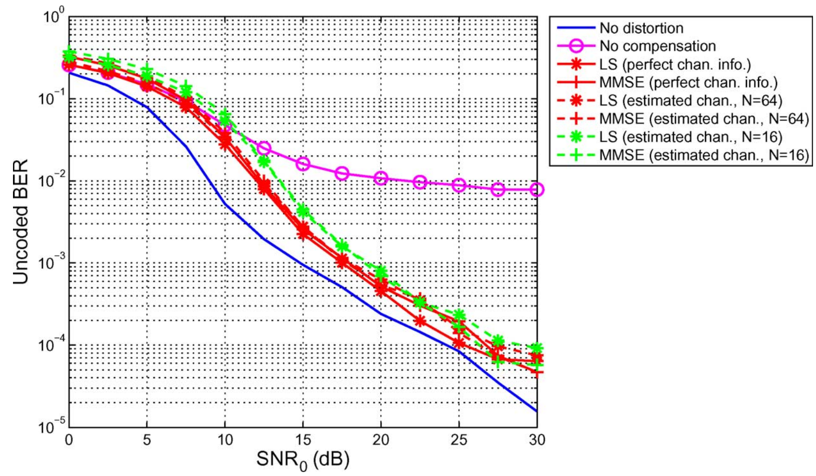

Fig. 10. Uncoded BER of the proposed scheme for $\alpha_1 = 56.23, \alpha_2 = 5.623, \alpha_3 = -7497.33, \sigma_{z,1}^2 = 10^{-12}$, and $\sigma_{z,2}^2 = 5 \times 10^{-4}$.

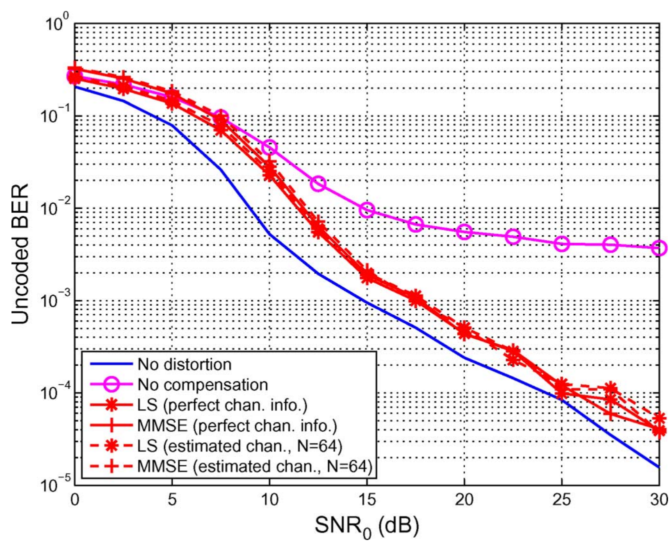

Fig. 11. Uncoded BER in the presence of two blocker signals when $\alpha_1 = 56.23, \alpha_2 = 5.623, \alpha_3 = -7497.33, \sigma_{z,1}^2 = 10^{-12}$, and $\sigma_{z,2}^2 = \sigma_{z,3}^2 = 2.5 \times 10^{-4}$.

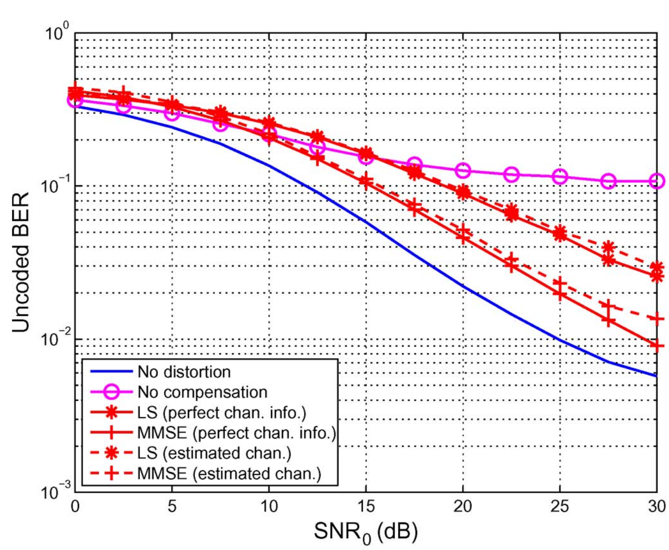

Fig. 12. Uncoded BER of OFDM systems for $\alpha_1 = 56.23, \alpha_2 = 5.623, \alpha_3 = -7497.33, \sigma_{z,1}^2 = 10^{-12}$, and $\sigma_{z,2}^2 = 5 \times 10^{-4}$.

Since $z_{i,R}(t)$ and $z_{i,I}(t)$ are independent of each other, the fourth and sixth moments of $z_i(t)$ are evaluated as

$$\begin{aligned}\mathbf{E}\left\{|z_i(t)|^4\right\} &= \mathbf{E}\left\{\left[z_{i,R}^2(t) + z_{i,I}^2(t)\right]^2\right\}\\ &= \mathbf{E}\left\{z_{i,R}^4(t)\right\} + 2\mathbf{E}\left\{z_{i,R}^2(t)\right\}\mathbf{E}\left\{z_{i,I}^2(t)\right\}\\ &\quad + \mathbf{E}\left\{z_{i,I}^4(t)\right\}\end{aligned} \tag{30}$$

and

$$\begin{aligned}\mathbf{E}\left\{|z_i(t)|^6\right\} &= \mathbf{E}\left\{\left[z_{i,R}^2(t) + z_{i,I}^2(t)\right]^3\right\}\\ &= \mathbf{E}\left\{z_{i,R}^6(t)\right\} + 3\mathbf{E}\left\{z_{i,R}^4(t)\right\}\mathbf{E}\left\{z_{i,I}^2(t)\right\}\\ &\quad + 3\mathbf{E}\left\{z_{i,R}^2(t)\right\}\mathbf{E}\left\{z_{i,I}^4(t)\right\} + \mathbf{E}\left\{z_{i,I}^6(t)\right\}.\end{aligned} \tag{31}$$

1) *Uniform Distribution*: Assume that $z_{i,R}(t)$ and $z_{i,I}(t)$ are uniformly distributed over $[-A_i, A_i]$. It is easy to verify that

$$\mathbf{E}\left\{z_{i,R}^2(t)\right\} = \mathbf{E}\left\{z_{i,I}^2(t)\right\} = \frac{1}{2A_i}\int_{-A_i}^{A_i} u^2 du = \frac{A_i^2}{3} \tag{32}$$

$$\mathbf{E}\left\{z_{i,R}^4(t)\right\} = \mathbf{E}\left\{z_{i,I}^4(t)\right\} = \frac{1}{2A_i}\int_{-A_i}^{A_i} u^4 du = \frac{A_i^4}{5} \tag{33}$$

$$\mathbf{E}\left\{z_{i,R}^6(t)\right\} = \mathbf{E}\left\{z_{i,I}^6(t)\right\} = \frac{1}{2A_i}\int_{-A_i}^{A_i} u^6 du = \frac{A_i^6}{7}. \tag{34}$$

By (29) and (32), we have

$$\sigma_{z,i}^2 = \mathbf{E}\left\{z_{i,R}^2(t)\right\} + \mathbf{E}\left\{z_{i,I}^2(t)\right\} = \frac{2A_i^2}{3}$$

which implies

$$A_i = \sqrt{\frac{3\sigma_{z,i}^2}{2}}. \tag{35}$$

By using (30)–(35), we have

$$\mathbf{E}\left\{|z_i(t)|^4\right\} = \frac{A_i^4}{5} + 2\left(\frac{A_i^2}{3}\right)^2 + \frac{A_i^4}{5} = \frac{28A_i^4}{45} = \frac{7}{5}\sigma_{z,i}^4$$

and

$$\begin{aligned}\mathbf{E}\left\{|z_i(t)|^6\right\} &= \frac{A_i^6}{7} + 3\left(\frac{A_i^4}{5}\right)\left(\frac{A_i^2}{3}\right) \\ &\quad + 3\left(\frac{A_i^2}{3}\right)\cdot\left(\frac{A_i^4}{5}\right) + \frac{A_i^6}{7} \\ &= \frac{24A_i^6}{35} = \frac{81}{35}\sigma_{z,i}^6.\end{aligned}$$

2) *Gaussian Distribution*: If $z_i(t)$ is circularly symmetric Gaussian distributed, its real and imaginary parts are i.i.d. Gaussian distributed with mean zero and variance $\sigma_{z,i}^2/2$. Thus,

$$\mathbf{E}\left\{z_{i,R}^2(t)\right\} = \mathbf{E}\left\{z_{i,I}^2(t)\right\} = \frac{\sigma_{z,i}^2}{2} \tag{36}$$

$$\mathbf{E}\left\{z_{i,R}^4(t)\right\} = \mathbf{E}\left\{z_{i,I}^4(t)\right\} = \frac{3\sigma_{z,i}^2}{4} \tag{37}$$

$$\mathbf{E}\left\{z_{i,R}^6(t)\right\} = \mathbf{E}\left\{z_{i,I}^6(t)\right\} = \frac{15\sigma_{z,i}^6}{8}. \tag{38}$$

By using (30), (31), and (36)–(38), we have

$$\mathbf{E}\left\{|z_i(t)|^4\right\} = \frac{3\sigma_{z,i}^2}{4} + 2\left(\frac{\sigma_{z,i}^2}{2}\right)^2 + \frac{3\sigma_{z,i}^2}{4} = 2\sigma_{z,i}^2$$

and

$$\begin{aligned}\mathbf{E}\left\{|z_i(t)|^6\right\} &= \frac{15\sigma_{z,i}^6}{8} + 3\left(\frac{3\sigma_{z,i}^2}{4}\right)\left(\frac{\sigma_{z,i}^2}{2}\right) \\ &\quad + 3\left(\frac{\sigma_{z,i}^2}{2}\right)\left(\frac{3\sigma_{z,i}^2}{4}\right) + \frac{15\sigma_{z,i}^6}{8} \\ &= 6\sigma_{z,i}^2.\end{aligned}$$

References

[1] Q. Zou, M. Mikhemar, and A. H. Sayed, "Digital compensation of RF nonlinearities in software-defined radios," in *Proc. IEEE Int. Conf. Acoust., Speech, Signal Process. (ICASSP)*, Apr. 2008, pp. 2921–2924.
[2] J. H. Reed, *Software Radio: A Modern Approach to Radio Engineering*. Upper Saddle River, NJ: Prentice-Hall, 2002.
[3] M. Dillinger, K. Madani, and N. Alonistioti, *Software Defined Radio: Architectures, Systems and Functions*. New York: Wiley, 2003.
[4] W. H. W. Tuttlebee, *Software Defined Radio: Baseband Technologies for 3G Handsets and Basestations*. New York: Wiley, 2004.
[5] P. Kenington, *RF and Baseband Techniques for Software Defined Radio*. Norwood, MA: Artech House, 2005.
[6] J. Bard and V. J. Kovarik, *Software Defined Radio: The Software Communications Architecture*. New York: Wiley, 2007.
[7] J. Mitola, III, "Cognitive radio: An integrated agent architecture for software defined radio," Ph.D. dissertation, Royal Inst. of Technol. (KTH), Stockholm, Sweden, May 2000.
[8] S. Haykin, "Cognitive radio: Brain-empowered wireless communications," *IEEE J. Sel. Areas Commun.*, vol. 23, no. 2, pp. 201–220, Feb. 2005.
[9] B. Razavi, *RF Microelectronics*. Englewood Cliffs, New Jersey: Prentice-Hall, 1998.
[10] A. A. Abidi, "Direct-conversion radio transceivers for digital communications," *IEEE J. Solid-State Circuits*, vol. 30, no. 12, pp. 1399–1410, Dec. 1995.
[11] R. Bagheri *et al.*, "An 800-MHz–6-GHz software-defined wireless receiver in 90-nm CMOS," *IEEE J. Solid-State Circuits*, vol. 41, no. 12, pp. 2860–2876, Dec. 2006.
[12] A. A. Abidi, "The path to the software-defined radio receiver," *IEEE J. Solid-State Circuits*, vol. 42, no. 5, pp. 954–966, May 2007.
[13] E. Biglieri, S. Barberis, and M. Catena, "Analysis and compensation of nonlinearities in digital transmission systems," *IEEE J. Sel. Areas Commun.*, vol. 6, no. 1, pp. 42–51, Jan. 1988.
[14] S. W. Nam and E. J. Powers, "On the linearization of Volterra nonlinear systems using third-order inverses in the digital frequency-domain," in *Proc. Int. Symp. Circuits Syst. (ISCAS)*, May 1990, pp. 407–410.
[15] D. Huang, H. Leung, and X. Huang, "A rational function based predistorter for high power amplifier," in *Proc. Int. Symp. Circuits Syst. (ISCAS)*, May 2004, pp. 1040–1043.
[16] Y. Ding and A. Sano, "Adaptive nonlinearity compensation for power amplifiers based on model-matching approach," in *Proc. 25th Chinese Control Conf.*, Aug. 2006, pp. 894–899.
[17] M. Valkama, A. S. H. Ghadam, L. Anttila, and M. Renfors, "Advanced digital signal processing techniques for compensation of nonlinear distortion in wideband multicarrier radio receivers," *IEEE Trans. Microw. Theory Tech.*, vol. 54, no. 6, pp. 2356–2366, Jun. 2006.
[18] U. Mengali, *Synchronization Techniques for Digital Receivers*. New York: Springer, 1997.
[19] A. H. Sayed, *Fundamentals of Adaptive Filtering*. New York: Wiley, 2003.
[20] D. Tse and P. Viswanath, *Fundamentals of Wireless Communication*. New York: Cambridge Univ. Press, 2005.
[21] S. M. Kay, *Fundamentals of Statistical Signal Processing: Estimation Theory*. Englewood Cliffs, New Jersey: Prentice-Hall, 1993, vol. I.

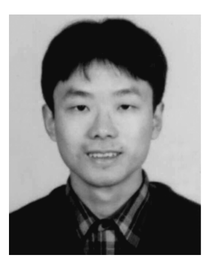

Qiyue Zou (S'06–M'09) received the B.Eng. and M.Eng. degrees in electrical and electronic engineering from Nanyang Technological University (NTU), Singapore, in 2001 and 2004, respectively, and the M.A. degree in mathematics and the Ph.D. degree in electrical engineering from University of California, Los Angeles (UCLA), in 2008.

From 2001 to 2004, he was with the Centre for Signal Processing, NTU, Singapore, working on statistical and array signal processing. He is currently with the WiLinx Corporation, San Diego, CA, working on ultrawideband communications. His research interests include signal processing, information theory, and wireless communications.

Dr. Zou received the Young Author Best Paper Award in 2007 from the IEEE Signal Processing Society.

Mohyee Mikhemar (S'99) received the B.S. and M.S. degrees with honors in electrical engineering from Ain Shams University, Cairo, Egypt, in 2000 and 2004, respectively. He is currently working toward the Ph.D. degree in the Electrical Engineering Department, University of California, Los Angeles

He has been an Intern with Broadcom, Irvine, CA, since April 2007. His research interests include software-defined and multimode radio system and circuit design, interference mitigation in CMOS RF front-ends, and employing DSP techniques to compensate for analog circuit imperfections.

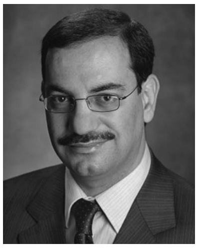

Ali H. Sayed (F'01) received the Ph.D. degree from Stanford University, Stanford, CA, in 1992.

He is Professor and Chairman of Electrical Engineering with the University of California, Los Angeles (UCLA), and Principal Investigator of the Adaptive Systems Laboratory. He has published widely, with more than 300 articles and four books, in the areas of statistical signal processing, estimation theory, adaptive filtering, signal processing for communications and wireless networking, and fast algorithms for large structured problems. He is coauthor of the textbook *Linear Estimation* (Prentice-Hall, 2000), of the research monograph *Indefinite Quadratic Estimation and Control* (SIAM, 1999), and coeditor of *Fast Algorithms for Matrices with Structure* (SIAM, 1999). He is also the author of the textbooks *Fundamentals of Adaptive Filtering* (Wiley, 2003), and *Adaptive Filters* (Wiley, 2008). He has contributed several encyclopedia and handbook articles.

Dr. Sayed is a Fellow of IEEE for his contributions to adaptive filtering and estimation algorithms. He has served on the editorial boards of the *IEEE Signal Processing Magazine*, the *European Signal Processing Journal*, the *International Journal on Adaptive Control and Signal Processing*, and the *SIAM Journal on Matrix Analysis and Applications*. He has also served as the Editor-in-Chief of the IEEE TRANSACTIONS ON SIGNAL PROCESSING (2003–2005), and the *EURASIP Journal on Advances in Signal Processing* (2006–2007). He is a member of the Signal Processing for Communications and the Signal Processing Theory and Methods Technical Committees of the IEEE Signal Processing Society. He has served on the Publications (2003–2005), Awards (2005), and Conference (2007–present) Boards of the IEEE Signal Processing Society. He also served on the Board of Governors of the IEEE Signal Processing Society (2007–2008) and is currently the Vice-President of Publications of the same Society. His work has received several recognitions including the 1996 IEEE Donald G. Fink Award, 2002 Best Paper Award from the IEEE Signal Processing Society, 2003 Kuwait Prize in Basic Sciences, 2005 Terman Award, 2005 Young Author Best Paper Award from the IEEE Signal Processing Society, and two Best Student Paper Awards at international meetings (1999 and 2001). He has served as a 2005 Distinguished Lecturer of the IEEE Signal Processing Society and as General Chairman of ICASSP 2008.